Machine learning approach for ball milling of alumina ceramics

Jungwon Yu
ETRI: Electronics and Telecommunications Research Institute
Raju Kati
KIT: Kumoh National Institute of Technology
So-Hyun Jin
KIT: Kumoh National Institute of Technology
Youngjae Lee
ETRI: Electronics and Telecommunications Research Institute
Hyun Kwuon Lee (hklee@kumoh.ac.kr)
KIT: Kumoh National Institute of Technology

Research Article

Keywords: Alumina, Wet ball mill, Machine learning, Polynomial regression analysis, Prediction interval, Parameter optimization

Posted Date: June 6th, 2022

DOI: https://doi.org/10.21203/rs.3.rs-1654928/v1

Machine learning approach for ball milling of alumina ceramics

Jungwon Yu[a], Kati Raju[b], So-Hyun Jin[b], Youngjae Lee[a], Hyun-Kwuon Lee[b,*]

[a] *Electronics and Telecommunications Research Institute, Daegu-Gyeongbuk Research Center, Daegu, 42994, South Korea*

[b] *School of Advanced Materials Science and Engineering, Kumoh National Institute of Technology, Gumi, Gyeongbuk, 39177, South Korea*

[*]Corresponding author:

H.-K. Lee, E-mail: hklee@kumoh.ac.kr;

Tel.: +82-54-478-7745; Fax: +82-54-478-7769

Abstract

In this work, machine learning (ML) approach based on polynomial regression was explored to analyze the optimal processing parameters and predict the target particle sizes for ball milling of alumina ceramics. Data points were experimentally obtained by measuring the particle sizes. Prediction interval (PI)-based optimization methods using polynomial regression analysis are proposed. As a first step, functional relations between the inputs and the responses are derived by applying the regression analysis. Later, based on these relations, objective functions to be maximized are defined by desirability approach. Finally, the proposed PI-based methods optimize both parameter points and intervals of the target mill for accomplishing user-specified target responses. The optimization results show that the PI-based point optimization methods can select and recommend statistically reliable optimized parameter points even though unique solutions for the objective functions do not exist. From the results of confirmation experiments, it is established that the optimized parameter points can produce desired particle sizes with quality responses quite similar to the target responses.

Keywords: Alumina; Wet ball mill; Machine learning; Polynomial regression analysis; Prediction interval; Parameter optimization.

1. Introduction

Machine learning (ML) methods have accelerated the scientific advancement in recent times since they are capable of processing of large amounts of data (big data) and their ability to select the optimal processing parameters more precisely. ML methods have been successfully applied in various fields including materials science, ceramics, glasses, and biomaterials [1−10]. These ML methods demonstrated their efficacy by the way the input data is processed and analyzed quantitatively. ML methods are successfully applied for the discovery of high-entropy ceramics [11] and alloys [12]. And also, for the prediction of permittivity for microwave dielectric ceramics [13], the melting temperature of ultra-high temperature ceramics [14] and the bending strength of silicon nitride ceramics [15].

Reliable, robust and accurate experimental input data is essential for ML since many methods are based on supervised learning approaches, in which the models are trained properly through the input data. It is also possible to predict the target values with a great accuracy through these ML methods and therefore selection of appropriate method is very important. Regression models are capable of predicting a continuous output and are generally used to predict numerical values based on input data. Regression models are trained by minimizing a loss function in a training data set. Regression-based ML methods have been applied efficaciously on different materials for the optimization and prediction of various properties [2−8]. However, ML methods have been applied very rarely to address the issues in the field of ceramics ball milling.

Ball mill is one of the most popular comminution machines used to produce desired reduced particle sizes and particle size distributions (PSDs) of starting powders [16−18]. It has been widely applied for fine grinding of materials in various fields including ceramics, mineral processing and electronics. Ball milling in general and wet ball milling in particular, is a

complex process governed by various processing parameters such as container and ball sizes, powder and ball loadings, milling speeds and times, slurry amounts, and so on [19−23]. Nevertheless, the quality of produced powders depends on the types and properties of starting powders. However, optimizing these processing parameters is absolutely needed in ceramics processing to achieve user-specified target values.

Numerous studies [24−36] have been made to optimize input parameters of ball milling processes, however, these studies have several limitations. For instance, most studies focused on optimizing milling parameters using only one quality response (mostly particle size, d_{50}). If, in addition to the d_{50}, the shape of PSDs is also considered as quality responses, multiple response optimization (MRO) problems should be dealt with. The methods based on the main effect plots cannot handle the MRO problems in which the trade-off between multiple responses should be treated. And also, most studies had little regard to solve such optimization problems in ball milling that desired target values for quality responses are set up. Main effect plots can maximize or minimize quality responses but cannot minimize the differences between the responses and their target values. Moreover, very few studies have attempted to optimize both milling parameter points and their intervals. The optimized parameter intervals can help to operate the target mill more flexibly by considering process uncertainties caused by measurement errors.

This paper proposes prediction interval (PI)-based optimization methods for optimizing a wet ball mill using polynomial regression analysis. The aim of the proposed methods is to optimize both parameter points and intervals of the target mill by solving such MRO problems that user-specified target values are set up for some quality responses. After deriving the regression functions from the collected dataset, establishing reasonable target values for particle sizes, and defining objective functions, the proposed PI-based optimization

methods were applied for optimizing both parameter points and intervals of the target mill. To verify the effectiveness of the optimized parameter points, confirmation experiments were also performed several times. Herein, we report on the applicability of polynomial regression-based ML approach for ball milling of alumina ceramics. Experimental data points were collected systematically via particle size analysis. Using this model, the optimal processing parameters can be selected and the target values can be predicted based on the input parameters. In particular, a quantitative analysis of the factors affecting the particle size was conducted. Although this study focuses on the ball milling of alumina ceramics, the new approach reported could be applied for other ceramic materials as well.

2. Experimental details

The value of d_{50} (y_1), and the values of width and skewness (y_2 and y_3) reflecting the shape of PSDs are employed as quality responses to assess milled alumina powders. The volume percent of slurry (x_1), solid content (x_2), milling speed (x_3), milling time (x_4), and ball size (x_5) are considered as key processing input parameters affecting these responses. 180 data samples were prepared, each of which consists of the settings of the five milling parameters (inputs) and the measured values of the three responses (outputs). More experimental details about the ball milling of alumina and data processing parameters can be found in our recent publication [37]. Fig. 1 summarizes the procedure for the proposed PI-based optimization methods, which is roughly divided into preliminary and optimization phases. In the preliminary phase, first, functional relations $\hat{y}_l(\mathbf{x})$, $l = 1,..., L$, between p inputs (i.e., processing parameters) and L outputs (i.e., quality responses) are derived by applying the regression analysis to an experimental dataset $\{(\mathbf{x}_i \in \Re^p; \mathbf{y}_i \in \Re^L)\}_{i=1}^n$. Second, based on the $\hat{y}_l(\mathbf{x})$, importance values of p inputs for each output are estimated by Monte Carlo (MC)-based method (Algorithm 1); the importance matrix $\mathbf{I}_{imp.} \in \Re^{L\times p}$ that consists of the estimated importance values can be employed

to prioritize processing parameters and to optimize parameter intervals. Third, objective functions $D(\mathbf{x})$ to be maximized for solving MRO problems are defined by desirability approach. In the optimization phase, first, the proposed point optimization method (Algorithm 2) is applied to $D(\mathbf{x})$ for obtaining statistically reliable optimized parameter points $\{\mathbf{x}^*_{(1)},...,\mathbf{x}^*_{(K')}\}$ to be recommended for the users (e.g., process operators and engineers). After that, the proposed interval optimization method (Algorithm 3) is used to find upper and lower bound vectors $\mathbf{x}^*_{LB}=[x^*_{LB,1},...,x^*_{LB,p}]^T$ and $\mathbf{x}^*_{UB}=[x^*_{UB,1},...,x^*_{UB,p}]^T$ that can define parameter intervals $[x^*_{LB,j}, x^*_{UB,j}]$, j = 1,..., p, enclosing an optimized point $\mathbf{x}^*_{(k)} \in \{\mathbf{x}^*_{(1)},...,\mathbf{x}^*_{(K')}\}$.

3. Polynomial regression analysis

Second-order polynomial regression analysis has been popularly used to optimize processing parameters in various industrial fields including powder processing using ball milling [29, 38−44], since it can construct regression models that can appropriately capture the nonlinearities contained in such experimental datasets with relatively low model complexity. Functional relations between p inputs x_1,..., x_p and lth output y_l (l = 1,..., L) are formulated by the regression analysis as follows:

$$y_l = f_l(\mathbf{x}\,|\,\boldsymbol{\beta}_l)+\varepsilon_l = \beta_0^l + \sum_{j=1}^{p}\beta_j^l x_j + \sum_{j<k}\beta_{jk}^l x_j x_k + \sum_{j=1}^{p}\beta_{jj}^l x_j^2 + \varepsilon_l \qquad (1)$$

where ε_l is an error term, β_0^l is an intercept, and β_j^l, β_{jk}^l, and β_{jj}^l are regression coefficients associated with linear, interaction, and quadratic terms, respectively. More details can be found in our recent publication [37]

The output of the lth regression function in eq. (1) for a new vector $\mathbf{x}_{\text{new}}$ = [$x_{\text{new},1}$,..., $x_{\text{new},p}$]^T can be calculated as $\hat{y}_l(\mathbf{x}_{\text{new}})=\mathbf{z}(\mathbf{x}_{\text{new}})^T\hat{\boldsymbol{\beta}}^l=\mathbf{z}_{\text{new}}^T\hat{\boldsymbol{\beta}}^l$, and its 100(1 − α)% PI, $[PI_{LB}^l(\mathbf{x}_{\text{new}}), PI_{UB}^l(\mathbf{x}_{\text{new}})]$, is calculated as

$$PI_{LB}^{l}(\mathbf{x}_{\text{new}}) = \hat{y}_l(\mathbf{x}_{\text{new}}) - t_{1-\alpha/2}(n-p')s_l\sqrt{1+\mathbf{z}_{\text{new}}^T(\mathbf{Z}^T\mathbf{Z})^{-1}\mathbf{z}_{\text{new}}}$$
$$PI_{UB}^{l}(\mathbf{x}_{\text{new}}) = \hat{y}_l(\mathbf{x}_{\text{new}}) + t_{1-\alpha/2}(n-p')s_l\sqrt{1+\mathbf{z}_{\text{new}}^T(\mathbf{Z}^T\mathbf{Z})^{-1}\mathbf{z}_{\text{new}}} \quad (2)$$

where α is significance level for PI, and $t_{1-\alpha/2}(n-p')$ is the $1-\alpha/2$ percentile of the t distribution $t(n-p')$.

3.1 Monte Carlo (MC)-based method for estimating importance values of inputs

In this work, MC-based method summarized in Algorithm 1 is used to estimate importance values of p inputs x_j (j = 1,..., p) for each output y_l (l = 1,..., L); this is a modified version of the method presented in [45,46]. First of all, after generating N uniform random vectors $\mathbf{x}^{(1)}$,..., $\mathbf{x}^{(N)}$ with p dimensions, these vectors are substituted into the lth regression function $\hat{y}_l(\mathbf{x}) = f_l(\mathbf{x}\,|\,\hat{\boldsymbol{\beta}}^l)$ to obtain N outputs $y_l^{(1)},..., y_l^{(N)}$, and their median $y_{l,\text{med}}$ is calculated. The random vectors can be partitioned into two sets as follows: $X_{\text{larger}}^{l} = \{\mathbf{x}^{(i)} |\, \hat{y}_l^{(i)} \geq y_{l,\text{med}}, i = 1,..., N\}$ and $X_{\text{smaller}}^{l} = \{\mathbf{x}^{(1)},..., \mathbf{x}^{(N)}\} \setminus X_{\text{larger}}^{l}$. And then, two empirical cumulative distribution functions (ECDFs), $F_{\text{larger}}^{l}(x_j)$ and $F_{\text{smaller}}^{l}(x_j)$ for each input x_j are estimated based on the jth elements of the vectors in X_{larger}^{l} and X_{smaller}^{l}, respectively. Finally, the total area of the region(s) surrounded by the two ECDFs are calculated numerically, and the calculated value is regarded as the importance value of x_j for y_l. Finishing the Algorithm 1, importance matrix $\mathbf{I}_{\text{imp.}} \in \Re^{L\times p}$ composed of the estimated importance values are returned.

4. Optimization of parameter points and intervals

4.1 Desirability approach

Desirability approach [47−49] has been commonly employed for defining objective functions for MRO problems in which multiple quality responses with different ranges are handled. Depending on whether a response y_l should be minimized, maximized or as close as possible to a target value $y_{l,\text{target}}$, different desirability functions are used, and these functions

transform the output value $\hat{y}_l(\mathbf{x})$ to have the range of 0 to 1. If there are user-specified target values for y_l, the following is used as its desirability function:

$$d_l\left(\hat{y}_l(\mathbf{x})\right)=\begin{cases}0 & \text{if } \hat{y}_l(\mathbf{x}) < y_{l,\min} \\ \left(\dfrac{\hat{y}_l(\mathbf{x})-y_{l,\min}}{y_{l,\text{target}}-y_{l,\min}}\right)^s & \text{if } y_{l,\min} \le \hat{y}_l(\mathbf{x}) \le y_{l,\text{target}} \\ \left(\dfrac{\hat{y}_l(\mathbf{x})-y_{l,\max}}{y_{l,\text{target}}-y_{l,\max}}\right)^t & \text{if } y_{l,\text{target}} \le \hat{y}_l(\mathbf{x}) \le y_{l,\max} \\ 0 & \text{if } \hat{y}_l(\mathbf{x}) > y_{l,\max}\end{cases} \tag{3}$$

where $y_{l,\min}$ and $y_{l,\max}$ are the lower and upper limits of y_l, respectively, both of which can be obtained from the observations $y_{1l},\ldots, y_{nl}$, $y_{l,\text{target}} \in [y_{l,\min}, y_{l,\max}]$ is a target value for y_l, and s and t are design values that determine the shape of eq. (3). If the lth response should be minimized, the following desirability function is used:

$$d_l\left(\hat{y}_l(\mathbf{x})\right)=\begin{cases}1 & \text{if } \hat{y}_l(\mathbf{x}) < y_{l,\min} \\ \left(\dfrac{y_{l,\max}-\hat{y}_l(\mathbf{x})}{y_{l,\max}-y_{l,\min}}\right)^t & \text{if } y_{l,\min} \le \hat{y}_l(\mathbf{x}) \le y_{l,\max} \\ 0 & \text{if } \hat{y}_l(\mathbf{x}) > y_{l,\max}\end{cases} \tag{4}$$

The desirability function used when the response should be maximized is similar to eq. (4), and thus omitted due to space constraints. In this paper, both design values of s and t in eqs. (3) and (4) are set to 1.

The following overall desirability $D(\mathbf{x})$, weighted geometric mean of $d_l(\cdot)$, $l = 1,\ldots, L$, are used as objective functions for MRO problems:

$$D(\mathbf{x})=\left(\prod_{l=1}^{L} d_l\left(\hat{y}_l(\mathbf{x})\right)^{w_l}\right)^{1/\sum_l w_l} \tag{5}$$

where w_l is a weight value assigned to lth response; in this paper, all weight values are set to 1.

4.2 PI-based method for optimizing parameter points

It should be noted that unique solutions do not exist in such MRO problems that some quality responses want to be equal to user-specified target values. That is, whenever executing optimization algorithms (e.g., quadratic programming and particle swarm optimization (PSO)) to maximize $D(\mathbf{x})$, different solutions are discovered each time. It is, therefore, essential to decide which of these different solutions to be selected and then recommended for users. Among these different solutions, the proposed PI-based point optimization method in Algorithm 2 selects statistically significant solutions (i.e., optimized parameter points) based on the lengths of their PIs. Here, it is assumed that as the length of PIs for a solution becomes shorter, its uncertainty is reduced from a statistical viewpoint. The proposed method is an advanced version of the method proposed in [50] so that it can be also applicable for MRO problems, and the significance of the different solutions is evaluated in terms of PIs instead of confidence intervals.

In the proposed method, firstly, different solutions $\mathbf{x}_k^*$, k = 1,..., K, are obtained by applying an optimization algorithm to maximize $D(\mathbf{x})$ multiple times. In this work, PSO [51−53] was applied to find these solutions. And then, the lengths of L PIs, $PI_k^l = PI_{UB}^l(\mathbf{x}_k^*) - PI_{LB}^l(\mathbf{x}_k^*)$, l = 1,..., L, associated with the kth solution $\mathbf{x}_k^*$ are calculated using eq. (2); the upper and lower limits $y_{l,\max}$ and $y_{l,\min}$ of y_l can be used to standardize the values of PI_k^l. Finally, PI_k, k = 1,..., K, obtained by summing all the standardized values PI_k^l, are sorted in ascending order (i.e., $PI_{(1)} < PI_{(2)} <$ ⊥), and then the K' solutions $\mathbf{x}_{(1)}^*,...,\mathbf{x}_{(K')}^*$ with the first K' PI_k are returned.

4.3 PI-based method for optimizing parameter intervals

To deal with the process uncertainties, in addition to an optimized parameter point $\mathbf{x}^* = [\, x_1^*,..., x_p^* \,]^T$, it is also necessary to obtain statistically meaningful optimized parameter

intervals $[x^*_{LB,j}, x^*_{UB,j}]$, j = 1,..., p, enclosing the point $\mathbf{x}^*$, i.e., $x^*_j \in [x^*_{LB,j}, x^*_{UB,j}], \forall j$. It is desirable that parameter points belonging to the domain restricted by these parameter intervals can achieve similar quality responses with those of $\mathbf{x}^*$ from a statistical view point.

In the p-dimensional input space, an hyper-rectangle (i.e., orthotope) that is centered at $\mathbf{x}^*$ and has 2^p vertices $\mathbf{v}_m \in \Re^p$, m = 1,..., 2^p, can be imagined. Fig. 2 shows the example of the hyper-rectangle with 8 (= 2^3) vertices defined in a three-dimensional input space. While redefining the hyper-rectangle by increasing the length of its edges gradually, one can discover the one defined immediately before any of output values $\hat{y}_l(\mathbf{v}_m)$, l = 1,..., L, start to depart from the PIs of $\mathbf{x}^*$, $[PI^l_{LB}(\mathbf{x}^*), PI^l_{UB}(\mathbf{x}^*)]$, l = 1,..., L. The parameter intervals can be easily obtained from the discovered hyper-rectangle. Weight values $\bar{W}_{lj}$ (j = 1,..., p, l = 1,..., L) calculated from the importance matrix $\mathbf{I}_{\text{imp.}}$ can be used to differentially increase the length of edges according to their relevant importance values; the larger the importance values, the shorter the length of the relevant edges.

In the proposed PI-based interval optimization method, first, the hyper-rectangle in which the length of the edges in parallel with the jth input direction is $2 \times \delta_l \bar{W}_{lj}$ are defined where δ_l is a small positive increment; this can be represented as a Cartesian product of p intervals as follows [54]: $\times_{j=1}^{p} [x^*_j - \delta_l \bar{W}_{lj}, x^*_j + \delta_l \bar{W}_{lj}]$, where × is the Cartesian product operator. Second, the 2^p vertices $\mathbf{v}_m \in \Re^p$ are organized into the vertex set $V = \{\mathbf{v}_m \in \Re^p \mid m = 1,..., 2^p\}$. While increasing the length of the edges, the elements of $\mathbf{v}_m$ that become larger than +1 (or smaller than −1) should be replaced by +1 (or −1). The reason for doing this is due to the fact that each element of input vector $\mathbf{x}$ in the regression functions $\hat{y}_l(\mathbf{x})$ must be always located in the range [−1, 1] by a data standardization, i.e., $\mathbf{x} \in [-1, 1]^p$. Third, after calculating the outputs $\hat{y}_l(\mathbf{v}_m)$,

the maximum value of δ_l that makes all the outputs to be included in the lth PI[$PI_{LB}^{l}(\mathbf{x}^*)$, $PI_{UB}^{l}(\mathbf{x}^*)$] is found by grid search. Fourth, after finding the maximum values of $\delta_l, \delta_l^{\max}$, for all l, the following upper and lower bound vectors $\mathbf{x}_{UB}^{l}$ and $\mathbf{x}_{LB}^{l}$, l = 1,..., L, are defined:

$$\mathbf{x}_{UB}^{l} = [x_1^* + \delta_l^{\max}\bar{W}_{l1}, ..., x_p^* + \delta_l^{\max}\bar{W}_{lp}]^T \text{ and } \mathbf{x}_{LB}^{l} = [x_1^* - \delta_l^{\max}\bar{W}_{l1}, ..., x_p^* - \delta_l^{\max}\bar{W}_{lp}]^T \quad (6)$$

In eq. (6), all the vector components larger than +1 (or smaller than −1) must be replaced by +1 (or −1). Based on $\mathbf{x}_{UB}^{l}$ and $\mathbf{x}_{LB}^{l}$, the L different hyper-rectangles can be defined as follows: $\times_{j=1}^{p}[x_{LB,j}^{l}, x_{UB,j}^{l}]$, l = 1,..., L. It is important to note that the L regions occupied by these L hyper-rectangles can be different from each other. Finally, the upper and lower bound vectors that can define the overlap between all the hyper-rectangles are obtained as follows:

$$\mathbf{x}_{UB}^{*} = [\min_l x_{UB,1}^{l}, ..., \min_l x_{UB,p}^{l}]^T \text{ and } \mathbf{x}_{LB}^{*} = [\max_l x_{LB,1}^{l}, ..., \max_l x_{LB,p}^{l}]^T \quad (7)$$

The vectors $\mathbf{x}_{UB}^{*}$ and $\mathbf{x}_{LB}^{*}$ consists of the upper and lower bounds of the optimized parameter intervals $[x_{LB,j}^{*}, x_{UB,j}^{*}]$, j = 1,..., p, for $\mathbf{x}^*$, respectively. Note that all the input points belonging to the overlap (i.e., $\mathbf{x} \in [\mathbf{x}_{LB}^{*}, \mathbf{x}_{UB}^{*}]$) satisfy the following condition: $\hat{y}_l(\mathbf{x}) \in [PI_{LB}^{l}(\mathbf{x}^*), PI_{UB}^{l}(\mathbf{x}^*)]$, $\forall l$. The proposed PI-based interval optimization method explained so far is summarized in Algorithm 3.

5. Results and discussion

5.1 Results of regression analysis

To derive regression functions between p = 5 inputs and L = 3 outputs, three full models in eq. (1) with p' = 21 regression coefficients are fitted to the 180 data pairs via the method of least squares; all the input values should be standardized to belong in the range [−1, 1] in advance. And then, statistically significant terms can be identified by testing whether the p-

values are smaller than 0.1 or not. Table 1 [37] summarizes the identified statistically significant linear, interaction, and quadratic terms for each of quality responses; this table allows to understand which terms have significant effects on the responses. For example, it is obvious that all input parameters but milling speed (x_3) affect the d_{50} (y_1) not only linearly but also nonlinearly; x_3 has only a linear effect on y_1. It can also be expected that the elements of the parameter pairs (x_1, x_4), (x_1, x_5), (x_2, x_4), and (x_4, x_5) interact with each other in determining the value of y_1.

The reduced models can be obtained by eliminating all the redundant terms except for those in Table 1 from the full models. The following regression functions can be derived by refitting the reduced models to the data pairs:

$$\begin{aligned}\hat{y}_1(\mathbf{x}) = & \underset{(.0031)}{.6023} + \underset{(.0013)}{.0046}\,x_1 + \underset{(.0012)}{.0078}\,x_2 - \underset{(.0012)}{.0052}\,x_3 - \underset{(.0014)}{.0216}\,x_4 + \underset{(.0012)}{.0083}\,x_5 \\ & + \underset{(.0016)}{.0047}\,x_1x_4 + \underset{(.0014)}{.0040}\,x_1x_5 + \underset{(.0016)}{.0034}\,x_2x_4 + \underset{(.0016)}{.0048}\,x_4x_5 \\ & - \underset{(.0023)}{.0056}\,x_1^2 + \underset{(.0023)}{.0043}\,x_2^2 + \underset{(.0024)}{.0051}\,x_4^2 + \underset{(.0026)}{.0164}\,x_5^2\end{aligned} \tag{8}$$

$$\begin{aligned}\hat{y}_2(\mathbf{x}) = & \underset{(.027)}{1.725} + \underset{(.012)}{.076}\,x_1 + \underset{(.012)}{.040}\,x_2 + \underset{(.012)}{.031}\,x_3 - \underset{(.014)}{.188}\,x_4 + \underset{(.012)}{.174}\,x_5 \\ & - \underset{(.014)}{.024}\,x_2x_3 + \underset{(.015)}{.060}\,x_3x_5 + \underset{(.025)}{.076}\,x_4^2 - \underset{(.027)}{.245}\,x_5^2\end{aligned} \tag{9}$$

$$\begin{aligned}\hat{y}_3(\mathbf{x}) = & \underset{(.0048)}{.3245} + \underset{(.0019)}{.0149}\,x_1 + \underset{(.0019)}{.0097}\,x_2 - \underset{(.0021)}{.0420}\,x_4 + \underset{(.0018)}{.0419}\,x_5 \\ & + \underset{(.0022)}{.0110}\,x_1x_5 + \underset{(.0022)}{.0056}\,x_2x_5 + \underset{(.0022)}{.0038}\,x_3x_5 \\ & + \underset{(.0035)}{.0086}\,x_2^2 - \underset{(.0035)}{.0066}\,x_3^2 + \underset{(.0037)}{.0153}\,x_4^2 - \underset{(.0040)}{.0069}\,x_5^2\end{aligned} \tag{10}$$

where the SEs of the estimated coefficients are presented in parentheses at the bottom of the coefficients. Table 2 lists performance indices such as root mean squared error (RMSE), R^2, adjusted R^2, and F-statistic of the full and reduced models. Since the number of coefficients to be estimated is decreased when reducing the complexity of the models, the degree of freedom for the error term ε_l (l = 1,..., 3) is increased, and thus the RMSE values can be decreased. In

the reduced models, the values of R^2 are smaller than those in the full models, but the values of adjusted R^2 are larger than or equal to those in the full models. This indicates that for the given dataset the generalization capabilities of the reduced models are better than the full models. In the case of F-statistic, its values have become larger after reducing the number of the coefficients, and thus it is valid to say that the reduced models are more statistically significant.

Fig. 3 shows response surfaces and contour plots visualizing the input-output relationships of the reduced model $\hat{y}_1(\mathbf{x})$ in eq. (8); as space is limited, those of $\hat{y}_2(\mathbf{x})$ and $\hat{y}_3(\mathbf{x})$ are not presented here. In Fig. 3, two variables at X and Y axes are relevant to the interaction terms in Table 1. By examining these figures carefully, it is possible to qualitatively understand how the two variables interact with each other for the response. As shown in Figs. 3 (a) and (e), and Figs. 3 (c) and (g), in the early stages of milling (i.e., when $x_4 \leq 8$ hours), the changes of x_1 and x_2 have little effect on y_1; when the value of x_4 is equal to 24 hours, the value of y_1 tends to be proportional to the values of x_1 and x_2. It is also observed that reduction rate in y_1 deteriorates with increasing the values of x_1 and x_2. In Figs. 3 (b) and (f), it can be seen that as the value of x_5 becomes larger, the change of x_1 has more effect on the value of y_1. Figs. 3 (d) and (h) show that the longer the milling time, the larger the performance differences with respect to the d_{50} between 3 mm and 10 mm balls.

To estimate the importance values of the five inputs, N = 50,000 uniform random vectors $\mathbf{x}^{(i)} \sim \mathbf{U}[-1, 1]^5$ are generated and substituted into eqs. (8)-(10). Figs. 4 (a)-(e) show the histograms of x_1,..., x_5 associated with the two sets X^1_{larger} and X^1_{smaller}, and Figs. 4 (f)-(j) describe the estimated ECDFs $F^1_{\text{larger}}(x_j)$ and $F^1_{\text{smaller}}(x_j)$, j = 1,..., 5; the histograms and the estimated ECDFs relevant to l = 2 and 3 are omitted due to space constraints. Fig. 5 depicts bar graphs illustrating the importance values of x_1,..., x_5 for y_1,..., y_3 estimated from the ECDFs in Figs. 4

(f)-(j). As can be seen in Fig. 5 (a), x_4 is the most important parameter for changing the value of y_1, and followed in order by x_5, x_2, x_3, and x_1. Figs. 5 (b) and (c) indicate that x_4, x_5, and x_1 make the first, second, and third largest contributions in determining the values of y_2 and y_3; the importance values of x_2 and x_3 for y_2 are similar to each other, but x_2 is more important parameter for y_3 than x_3.

5.2 Results of optimization

After appointing proper desirability function $d_l(\cdot)$, l = 1,..., 3, to each of the functions in eqs. (8)-(10), an overall desirability function $D(\mathbf{x})$ used as an objective function can be defined by eq. (5). Since some desired target values are set for the value of the d_{50} (y_1), eq. (3) is employed for $d_1(\cdot)$; in general, width (y_2) and skewness (y_3) are required to be minimized, eq. (4) is used for $d_2(\cdot)$ and $d_3(\cdot)$.

Table 3 lists the optimization results of applying Algorithm 2 for maximizing $D(\mathbf{x})$ when the following target values were set up for the three responses and the parameter value of x_5 was constrained to 3 mm: $y_{1,\text{target}}$ = 0.58 μm, $y_{2,\text{target}}$ = 'min', and $y_{3,\text{target}}$ = 'min'. Here, the goal is to find the parameter points that can produce the following milled powder: its PSD is centered at the desired value of d_{50}, and at the same time, its width and both sides are as narrow and symmetrical as possible, respectively. The reason why the ball size (x_5) was restricted to be 3 mm is that it is a discrete input parameter, and thus its optimized values (e.g., $x_5^* = 4.73$) without the constrained condition cannot be used in practice. In Algorithm 2, the values of α, K, and K' are set to 0.01, 100, and 10, respectively. In Table 3, the optimized parameter points and their model outputs are summarized in the second to sixth columns and the seventh to ninth columns, respectively; the 99% PIs enclosing the outputs are also presented at the bottom of them. As listed in the table, the outputs of $\mathbf{x}_{(1)}^*, ..., \mathbf{x}_{(10)}^*$ are the same or very similar to each other, but the optimized parameter values of x_2^* and x_3^* in $\mathbf{x}_{(1)}^*$ and $\mathbf{x}_{(2)}^*$ are quite different from those of

others; this is due to the fact that since there are infinitely many input points that can achieve the target value $y_{1,\text{target}} = 0.58$ μm (see Fig. 3 (e)), optimization algorithms cannot find a unique solution. The optimized parameter intervals by Algorithm 3 with $\alpha = 0.01$ are presented at the bottom of the parameter values in $\mathbf{x}^*_{(1)}$ and $\mathbf{x}^*_{(3)}$ marked with boldface; the upper and lower bound vectors $\mathbf{x}^*_{UB}$ and $\mathbf{x}^*_{LB}$ for $\mathbf{x}^*_{(1)}$ are $[23.55, 70.00, 70.00, 24.00, 4.70]^T$ and $[20.00, 55.09, 61.77, 19.12, 3.00]^T$, respectively. Fig. 6 shows the contour plots of the regression function $\hat{y}_1(\mathbf{x})$ at which the first solution $\mathbf{x}^*_{(1)}$ and the input region defined by its optimum parameter intervals are indicated by red asterisks and dashed black lines, respectively. In these plots, it should be noted that the model outputs of the input vectors included in the region are very close to $y_{1,\text{target}} = 0.58$ μm. This suggests that the optimized intervals allow to know the tolerable setting errors of each parameter, and depending on field situations, it is also possible to flexibly adjust its values within the region. Table 4 summarizes the results of applying Algorithm 2 to the optimization problem with the target values $y_{1,\text{target}} = 0.60$ μm, $y_{2,\text{target}}$ = 'min', and $y_{3,\text{target}}$ = 'min', and with the equality constraint $x_5 = 3$ mm. As presented in the table, although the values of x_2^* and x_4^* in $\mathbf{x}^*_{(9)}$ are markedly different from those in others, all the outputs are the same or quite similar. The parameter intervals optimized by Algorithm 3 are indicated at the bottom of the parameter values in $\mathbf{x}^*_{(1)}$ and $\mathbf{x}^*_{(9)}$.

The productivity of the target mill is directly related with such input parameters as solid content (x_2), milling speed (x_3) and milling time (x_4) [55]. The solid content determines the amount of produced final powders, and milling speed and time are relevant to the amount of electrical energy consumption (i.e., production costs). Among the $K' = 10$ solutions listed in Tables 3 and 4, process operators and engineers can select and use appropriate solutions in consideration of the productivity. In Table 3, to satisfy the target values, and at the same time

to produce the larger amount of milled powders, $\mathbf{x}^*_{(1)}$ or $\mathbf{x}^*_{(2)}$ with higher value of x_2 can be used. The values of x_2 in $\mathbf{x}^*_{(1)}$ and $\mathbf{x}^*_{(2)}$ are about 10 wt% higher than those of others, but all the values of x_1 and x_4 in Table 3 are extremely similar to each other. However, if $\mathbf{x}^*_{(1)}$ or $\mathbf{x}^*_{(2)}$ is used, the container should be rotated with higher milling speed (i.e., x^*_3 = 70 %), and thus the amount of the energy consumption increases. In Table 4, to attain the target values and to reduce production time simultaneously, $\mathbf{x}^*_{(9)}$ can be used; it can save the time by 3.47 hours compared to $\mathbf{x}^*_{(1)}$. However, the value of x_2 in $\mathbf{x}^*_{(9)}$ is 9.33 wt% lower than that in $\mathbf{x}^*_{(1)}$, and thus the amount of produced powders by $\mathbf{x}^*_{(9)}$ will be smaller than $\mathbf{x}^*_{(1)}$.

5.3 Results of confirmation experiments

To verify the effectiveness of the optimized parameter points, confirmation experiments via the same steps as explained in previous section were performed based on $\mathbf{x}^*_{(1)}$ and $\mathbf{x}^*_{(3)}$ in Table 3, and $\mathbf{x}^*_{(1)}$ and $\mathbf{x}^*_{(9)}$ in Table 4. In these experiments, the milling parameters were set up in accordance with the optimized points, the final powders were produced, and then their three quality responses were measured. Considering the process uncertainties, the same experiments were repeated four times for each of the four optimized parameter points.

Tables 5 and 6 list the measured quality responses from the four milled powders by the optimized points $\mathbf{x}^*_{(1)}$ and $\mathbf{x}^*_{(3)}$ in Table 3, respectively; the averaged values of the measured responses are also summarized at the last row in each table. Figs. 7 (a) and (b) show the PSDs of the four milled powders in Tables 5 and 6, respectively. In Table 5, the measured values of d_{50} from the 1st and 2nd powders are 0.603 μm and 0.604 μm, approximately 0.02 μm lower than its target value; their measured values of y_2 and y_3 are smaller than the model outputs $\hat{y}_2(\mathbf{x}^*_{(1)})$ = 1.102 and $\hat{y}_3(\mathbf{x}^*_{(1)})$ = 0.239, respectively. The measured values of d_{50} from 3rd and 4th

powders are similar with its target value and their values of y_2 and y_3 are also smaller than the model outputs. In Table 6, the differences between the measured values of y_1 and its target value are less than 0.013 μm, and the smaller values of y_2 and y_3 than the outputs $\hat{y}_2(\mathbf{x}^*_{(3)}) =$ 1.106 and $\hat{y}_3(\mathbf{x}^*_{(3)}) =$ 0.245 have been obtained. Since all the measured responses in Tables 5 and 6 belong to the PIs in Table 3, it can be understood that the procedure in Fig. 1 can achieve the statistically reliable results of optimization. The average values of the responses in Tables 5 and 6 differ in the d_{50}, width, and skewness by 0.01 μm, 0.035, and 0.009, respectively; since $\mathbf{x}^*_{(1)}$ and $\mathbf{x}^*_{(3)}$ get the similar measured responses to each other, it seems reasonable to suppose that either one can be used to produce the final powder satisfied with the target values.

Tables 7 and 8 summarize the measured responses of the four powders obtained by $\mathbf{x}^*_{(1)}$ and $\mathbf{x}^*_{(9)}$ in Table 4, respectively. It can be confirmed that all the responses are included in the PIs in Table 4. The differences in the averaged values of d_{50}, width, and skewness between are 0.008, 0.007, and 0.003, respectively; these are negligible taking the process uncertainties into account. Figs. 8 (a) and (b) present the PSDs relevant to the four powders in Tables 7 and 8, respectively. As can be viewed from these figures, the PSDs measured by the four repeated experiments are extremely similar in shape; the shape of PSDs shown in each of the figures are also quite similar to each other.

6. Conclusions

In this study, ML approach based on polynomial regression was introduced to quantitatively analyze the optimal processing parameters and predict the target particle sizes for ball milling of alumina ceramics. Median particle size, width and skewness of PSDs for milled powders were regarded as quality responses. The volume percent of slurry, solid content, milling speed, milling time, and ball size were considered as key input parameters to be

optimized. PI-based point and interval optimization methods using polynomial regression analysis were proposed here. After deriving the functional relations between the inputs and the responses, and defining objective functions for solving MRO problems by desirability approach, the proposed methods were used to optimize both parameter points and intervals for accomplishing user-specified target responses. The optimization results showed that the proposed point optimization method can select and recommend statistically reliable optimized parameter points even though unique solutions for the objective functions do not exist. These results are established by additional confirmation experiments. Finally, although this study emphasized on the ball milling of alumina ceramics, the new approach reported herein could be applicable for other ceramic materials.

References

[1] J. Schmidt, M. R. G. Marques, S. Botti, M. A. L. Marques, Recent advances and applications of machine learning in solid-state materials science, npj Comput. Mater. 5 (2019) 83.

[2] K. Yang, X. Xu, B. Yang, B. Cook, H. Ramos, N. M. A. Krishnan, M. M. Smedskjaer, C. Hoover, M. Bauchy, Predicting the Young's modulus of silicate glasses using high-throughput molecular dynamics simulations and machine learning, Sci. Rep. 9 (2019) 8739.

[3] H. Liu, T. Zhang, N. M. A. Krishnan, M. M. Smedskjaer, J. V. Ryan, S. Gin, M. Bauchy, Predicting the dissolution kinetics of silicate glasses by topology-informed machine learning, npj Mater. Degrad. 3 (2019) 32.

[4] J. Wei, X. Chu, X.-Y. Sun, K. Xu, H.-X. Deng, J. Chen, Z. Wei, M. Lei, Machine learning in materials science, Infomat 1 (2019) 338–358.

[5] H. Liu, Z. Fu, K. Yang, X. Xu, M. Bauchy, Machine learning for glass science and engineering: A review, J. Non-Cryst. Solids: X 4 (2019) 100036.

[6] H. Yang, Z. Zhang, J. Zhang, X. C. Zeng, Machine learning and artificial neural network prediction of interfacial thermal resistance between graphene and hexagonal boron nitride, Nanoscale, 10 (2018) 19092.

[7] J. He, J. Li, C. Liu, C. Wang, Y. Zhang, C. Wen, D. Xue, J. Cao, Y. Su, L. Qiao, Y. Bai, Machine learning identified materials descriptors for ferroelectricity, Acta Mater. 209 (2021) 116815.

[8] J. Kerner, A. Dogan, H. V. Recum, Machine learning and big data provide crucial insight for future biomaterials discovery and research, Acta Biomater. 130 (2021) 54–65.

[9] J. F. Rodrigues Jr, L. Florea, M. C. F. de Oliveira, D. Diamond, O. N. Oliveira Jr, Big data and machine learning for materials science, Discover Materials 1 (2021)12.

[10] Y. Liu, C. Niu, Z. Wang, Y. Gan, Y. Zhu, S. Sun, T. Shen, Machine learning in materials genome initiative: A review, J. Mater. Sci. Technol. 57 (2020) 113–122.

[11] K. Kaufmann, D. Maryanovsky, W. M. Mellor, C. Zhu, A. S. Rosengarten, T. J. Harrington, C. Oses, C. Toher, S. Curtarolo, K. S. Vecchio, Discovery of high-entropy ceramics via machine learning, npj Comput. Mater. 6 (2020) 42.

[12] K. Kaufmann, K. S. Vecchio, Searching for high entropy alloys: A machine learning approach, Acta Mater. 198 (2020) 178–222.

[13] J. Qin, Z. Liu, M. Ma, Y. Li, Machine learning approaches for permittivity prediction and rational design of microwave dielectric ceramics, J. Materiomics 7 (2021) 1284–1293.

[14] N. Qu, Y. Liu, M. Liao, Z. Lai, F. Zhou, P. Cui, T. Han, D. Yang, J. Zhu, Ultra-high temperature ceramics melting temperature prediction via machine learning, Ceram. Int. 45 (2019) 18551–18555.

[15] P. Yang, S. Wu, H. Wu, D. Lu, W. Zou, L. Chu, Y. Shao, S. Wu, Prediction of bending strength of Si_3N_4 using machine learning, Ceram. Int. 47 (2021) 23919–23926.

[16] J.S. Reed, Principles of Ceramics Processing, 2nd ed., John Wiley & Sons, Inc., New York, 1995.

[17] C. Suryanarayana, Mechanical alloying and milling, Prog. Mater. Sci 46 (2001) 1–184.

[18] R. Janot, D. Guérard, Ball-milling in liquid media: Applications to the preparation of anodic materials for lithium-ion batteries, Prog. Mater. Sci. 50 (2005) 1–92.

[19] C. Frances, C. Laguerie, Fine wet grinding of an alumina hydrate in a ball mill, Powder Technol. 99 (1998) 147–153.

[20] H. Shin, S. Lee, H.S. Jung, J.B. Kim, Effect of ball size and powder loading on the milling efficiency of a laboratory-scale wet ball mill, Ceram. Int. 39 (2013) 8963–8968.

[21] F.K. Mulenga, M.H. Moys, Effects of slurry pool volume on milling efficiency, Powder Technol. 256 (2014) 428–435.

[22] A. Wagih, A. Fathy, A.M. Kabeel, Optimum milling parameters for production of highly uniform metal-matrix nanocomposites with improved mechanical properties, Adv. Powder Technol. 29 (2018) 2527–2537.

[23] H.M. Oh, Y.J. Park, H.N. Kim, J.W. Ko, H.K. Lee, Effect of milling ball size on the densification and optical properties of transparent Y_2O_3 ceramics, Ceram. Int. 47 (2021) 4681–4687.

[24] T.H. Hou, C.H. Su, W.L. Liu, Parameters optimization of a nano-particle wet milling process using the Taguchi method, response surface method and genetic algorithm, Powder Technol. 173 (2007) 153–162.

[25] F.L. Zhang, M. Zhu, C.Y. Wang, Parameters optimization in the planetary ball milling of nanostructured tungsten carbide/cobalt powder, Int. J. Refract. Met. Hard Mat. 26 (2008) 329–333.

[26] J. Ma, S.G. Zhu, C.X. Wu, M.L. Zhang, Application of back-propagation neural network technique to high-energy planetary ball milling process for synthesizing nanocomposite WC-MgO powders, Mater. Des. 30 (2009) 2867–2874.

[27] A. Charkhi, H. Kazemian, M. Kazemeini, Optimized experimental design for natural clinoptilolite zeolite ball milling to produce nano powders, Powder Technol. 203 (2010) 389–396.

[28] O.Y. Toraman, D. Katırcıoglu, A study on the effect of process parameters in stirred ball mill, Adv. Powder Technol. 22 (2011) 26–30.

[29] O. Celep, N. Aslan, İ. Alp, G. Taşdemir, Optimization of some parameters of stirred mill for ultra-fine grinding of refractory Au/Ag ores, Powder Technol. 208 (2011) 121–127.

[30] A. Ebadnejad, G.R. Karimi, H. Dehghani, Application of response surface methodology for modeling of ball mills in copper sulphide ore grinding, Powder Technol. 245 (2013) 292–296.

[31] A. Canakci, F. Erdemir, T. Varol, A. Patir, Determining the effect of process parameters on particle size in mechanical milling using the Taguchi method: measurement and analysis, Measurement 46 (2013) 3532–3540.

[32] A.G. Patil, S. Anandhan, Influence of planetary ball milling parameters on the mechano-chemical activation of fly ash, Powder Technol. 281 (2015) 151–158.

[33] F. Erdemir, Study on particle size and X-ray peak area ratios in high energy ball milling and optimization of the milling parameters using response surface method, Measurement 112 (2017) 53–60.

[34] S. Petrović, L. Rožić, V. Jović, S. Stojadinović, B. Grbić, N. Radić, J. Lamovec, R. Vasilić, Optimization of a nanoparticle ball milling process parameters using the response surface method, Adv. Powder Technol. 29 (2018) 2129–2139.

[35] H. Hajji, S. Nasr, N. Millot, E.B. Salem, Study of the effect of milling parameters on mechanosynthesis of hydroxyfluorapatite using the Taguchi method, Powder Technol. 356 (2019) 566–580.

[36] T. Santosh, K.S. Rahul, C. Eswaraiah, D.S. Rao, R. Venugopal, Optimization of stirred mill parameters for fine grinding of PGE bearing chromite ore, Part. Sci. Technol. 9 (2020) 1–13.

[37] J. Wu, S.-H. Jin, K. Raju, Y. Lee, H.-K. Lee, Analysis of individual and interaction effects of processing parameters on wet grinding performance in ball milling of alumina ceramics using statistical methods, Ceram. Int. 47 (2021) 31202–31213.

[38] N.R. Draper, H. Smith, Applied regression analysis, 3rd ed., John Wiley & Sons, Inc., 1998.

[39] D.C. Montgomery, E.A. Peck, G.G. Vining, Introduction to linear regression analysis, 5th ed., John Wiley & Sons, Inc., New Jersey, 2012.

[40] A. Aggarwal, H. Singh, P. Kumar, M. Singh, Optimizing power consumption for CNC turned parts using response surface methodology and Taguchi's technique-a comparative analysis. J. Mater. Process. Technol. 200 (2008) 373–384.

[41] N. Costa, J. Garcia, Using a multiple response optimization approach to optimize the coefficient of performance, Appl. Therm. Eng. 96 (2016) 137–143.

[42] H. Mostafanezhad, H.G. Menghari, S. Esmaeili, E.M. Shirkharkolaee, Optimization of two-point incremental forming process of AA1050 through response surface methodology, Measurement 127 (2018) 21–28.

[43] M.K. Parida, H. Joardar, A.K. Rout, I. Routaray, B.P. Mishra, Multiple response optimizations to improve performance and reduce emissions of Argemone Mexicana biodiesel-diesel blends in a VCR engine, Appl. Therm. Eng. 148 (2019) 1454–1466.

[44] V.S. Yaliwal, N.R. Banapurmath, V.N. Gaitonde, M.D. Malipatil, Simultaneous optimization of multiple operating engine parameters of a biodiesel-producer gas operated compression ignition (CI) engine coupled with hydrogen using response surface methodology, Renew. Energy 139 (2019) 944–959.

[45] B. Deng, Y. Shi, T. Yu, C. Kang, P. Zhao, Multi-response parameter interval sensitivity and optimization for the composite tape winding process, Materials 11 (2018) 220.

[46] Z. Chen, Y. Shi, X. Lin, T. Yu, P. Zhao, C. Kang, X. He, H. Li, Analysis and optimization of process parameter intervals for surface quality in polishing Ti-6Al-4V blisk blade, Results Phys. 12 (2019) 870–877.

[47] E.D. Castillo, Process optimization: a statistical approach, Springer Science & Business Media, 2007.

[48] L.V. Candioti, M.M. De Zan, M.S. Cámara, H.C. Goicoechea, Experimental design and multiple response optimization using the desirability function in analytical methods development, Talanta 124 (2014) 123–138.

[49] S. Mohanty, A. Mishra, B.K. Nanda, B.C. Routara, Multi-objective parametric optimization of nano powder mixed electrical discharge machining of $AlSiC_p$ using response surface methodology and particle swarm optimization, Alex. Eng. J. 57 (2018) 609–619.

[50] J. Yu, S. Yang, J. Kim, Y. Lee, K.T. Lim, S. Kim, S.-S. Ryu, H. Jeong, A confidence interval-based process optimization method using second-order polynomial regression analysis, Processes 8 (2020) 1206.

[51] R. Eberhart, J. Kennedy, Particle swarm optimization, In Proceedings of the IEEE international conference on neural networks 4 (1995) 1942–1948.

[52] A.P. Engelbrecht, Computational intelligence: an introduction, John Wiley & Sons, 2007.

[53] Y. Del Valle, G.K. Venayagamoorthy, S. Mohagheghi, J.C. Hernandez, R.G. Harley, Particle swarm optimization: basic concepts, variants and applications in power systems, IEEE Trans. Evol. Comput. 12 (2008) 171–195.

[54] T. Dayar, M.C. Orhan, Cartesian product partitioning of multi-dimensional reachable state spaces, Probab. Eng. Inform. Sci. 30 (2016) 413–430.

[55] S.S. Razavi-Tousi, J.A. Szpunar, Effect of ball size on steady state of aluminum powder and efficiency of impacts during milling, Powder Technol. 284 (2015) 149–158.

Statements & Declarations

Funding

This work was supported by the Ministry of Trade, Industry and Energy (MOTIE) and the Korea Evaluation Institute of Industrial Technology (KEIT) research funding (Grant No. 20003891 & 20004367), and in part by Electronics and Telecommunications Research Institute (ETRI) grant funded by the Korean government [22ZD1120, Regional Industry ICT

Convergence Technology Advancement and Support Project in Daegu-GyeongBuk].

Competing interests

The authors declare that they have no known competing financial interests or personal relationships that could have appeared to influence the work reported in this paper.

Availability of data and materials

All data generated or mentioned in this study are included in this published article.

Code availability

No code was provided in this manuscript

Ethics approval

This study does not involve ethical issues.

Consent to participate

All authors agreed to participate in this research.

Consent for publication

All authors have reviewed the final version of manuscript and approve it for publication.

Algorithms

Algorithm 1. MC-based method for estimating importance values of p inputs.

Input: Regression functions $\hat{y}_l(\mathbf{x}) = f_l(\mathbf{x} \mid \hat{\boldsymbol{\beta}}^l)$, $l = 1,..., L$

$\mathbf{I}_{\text{imp.}} \leftarrow L$ by p empty matrix

Generate N uniform random vectors $\mathbf{x}^{(i)} \in \Re^p \sim \mathbf{U}[-1, 1]^p$, $i = 1,..., N$
for l from 1 to L
  Calculate N output values $\hat{y}_l^{(i)} = f_l(\mathbf{x}^{(i)} \mid \hat{\boldsymbol{\beta}}^l)$, $i = 1,..., N$
  $y_{l,\text{med}} \leftarrow \text{median}(\hat{y}_l^{(1)},..., \hat{y}_l^{(N)})$
  $X^l_{\text{larger}} \leftarrow \{\mathbf{x}^{(i)} \mid \hat{y}_l^{(i)} \geq y_{l,\text{med}}, i = 1,..., N\}$, and $X^l_{\text{smaller}} \leftarrow \{\mathbf{x}^{(1)},..., \mathbf{x}^{(N)}\} \setminus X^l_{\text{larger}}$
  for j from 1 to p
    Estimate two ECDFs $F^l_{\text{larger}}(x_j)$ and $F^l_{\text{smaller}}(x_j)$ based on the jth elements of $\mathbf{x}^{(i)}$ in X^l_{larger} and X^l_{smaller}, respectively
    Calculate the *total area* of the region(s) surrounded by the ECDFs numerically
    $\mathbf{I}_{\text{imp.}}(l, j) \leftarrow$ *total area*
  end for j
end for l
return $\mathbf{I}_{\text{imp.}}$

Algorithm 2. Proposed PI-based method for optimizing parameter points.

Input: Regression functions $\hat{y}_l(\mathbf{x})$, $l = 1,..., L$, and objective function $D(\mathbf{x})$

$\alpha \leftarrow$ significant level for PI
$y_{l,\max}, y_{l,\min} \leftarrow$ upper and lower bounds for lth output y_l
$K \leftarrow$ # of repetitions of applying an optimization algorithm to $D(\mathbf{x})$
$K' \leftarrow$ # of solutions to be recommended (where $K' < K$)

for k from 1 to K
  Find a solution $\mathbf{x}_k^*$ using an optimization algorithm to maximize $D(\mathbf{x})$:

$$\mathbf{x}_k^* \leftarrow \arg\max_{\mathbf{x}\in[-1,1]^p} D(\mathbf{x})$$

  for l from 1 to L
    Calculate the length of lth PI for $\mathbf{x}_k^*$ using eq. (4):

$$PI_k^l \leftarrow PI_{UB}^l(\mathbf{x}_k^*) - PI_{LB}^l(\mathbf{x}_k^*)$$

  end for l
end for k
$PI_k \leftarrow \sum_{l=1}^{L} PI_k^l / (y_{l,\max} - y_{l,\min})$, $k = 1,..., K$
Sort PI_k in ascending order, i.e., $PI_{(1)} < PI_{(2)} <$L
return $\{\mathbf{x}_{(1)}^*, \mathbf{x}_{(2)}^*, ..., \mathbf{x}_{(K')}^*\}$

Algorithm 3. Proposed PI-based method for optimizing parameter intervals.

Input: Regression functions $\hat{y}_l(\mathbf{x})$, $l = 1,..., L$, a solution $\mathbf{x}^*$, and
importance matrix $\mathbf{I}_{\text{imp.}} \in \Re^{L\times p}$

$\alpha \leftarrow$ significant level for PI
$\mathbf{W} \leftarrow \mathbf{J}_{L\times p} - \mathbf{I}_{\text{imp.}}$ //$\mathbf{J}_{L\times p}$: L by p matrix of ones
$\delta_l \leftarrow 0$, $l = 1,..., L$

for l from 1 to L
Calculate weights for p inputs:
$$\bar{W}_{lj} \leftarrow W_{lj} \Big/ \sum\nolimits_j W_{lj}, j = 1,..., p \quad //W_{lj}\text{: } (l, j)\text{th element of } \mathbf{W}$$
Obtain prediction interval $[PI^l_{LB}(\mathbf{x}^*), PI^l_{UB}(\mathbf{x}^*)]$ for $\mathbf{x}^*$ using eq. (4)
while $\hat{y}_l(\mathbf{v}_m) \in [PI^l_{LB}(\mathbf{x}^*), PI^l_{UB}(\mathbf{x}^*)]$, $m = 1,..., 2^p$
$\delta_l \leftarrow \delta_l + 0.01$
Define the p-dimensional hyper-rectangle:
$$\times_{j=1}^{p}[x_j^* - \delta_l \bar{W}_{lj}, x_j^* + \delta_l \bar{W}_{lj}]$$
Organize the vertices of the hyper-rectangle into the vertex set V:
$$V \leftarrow \{\mathbf{v}_m \in \Re^p \mid m = 1,..., 2^p\}$$
if $v_{mj} > 1$, $m = 1,..., 2^p, j = 1,..., p$ **then** $v_{mj} \leftarrow 1$ **end if**
if $v_{mj} < -1$, $m = 1,..., 2^p, j = 1,..., p$ **then** $v_{mj} \leftarrow -1$ **end if**
Calculate the outputs $\hat{y}_l(\mathbf{v}_m)$ for $\mathbf{v}_m$, $m = 1,..., 2^p$
end while
$\delta_l^{\max} \leftarrow \delta_l - 0.01$
$\mathbf{x}^l_{UB} \leftarrow [x_1^* + \delta_l^{\max}\bar{W}_{l1},..., x_p^* + \delta_l^{\max}\bar{W}_{lp}]^T$, and $\mathbf{x}^l_{LB} \leftarrow [x_1^* - \delta_l^{\max}\bar{W}_{l1},..., x_p^* - \delta_l^{\max}\bar{W}_{lp}]^T$
if $x^l_{UB,j} > 1, j = 1,..., p$ **then** $x^l_{UB,j} \leftarrow 1$ **end if**
if $x^l_{LB,j} < -1, j = 1,..., p$ **then** $x^l_{UB,j} \leftarrow -1$ **end if**
end for l
$\mathbf{x}^*_{UB} \leftarrow [\min_l x^l_{UB,1},..., \min_l x^l_{UB,p}]^T$, and $\mathbf{x}^*_{LB} \leftarrow [\max_l x^l_{LB,1},..., \max_l x^l_{LB,p}]^T$
return $\mathbf{x}^*_{UB}$ and $\mathbf{x}^*_{LB}$

Figures

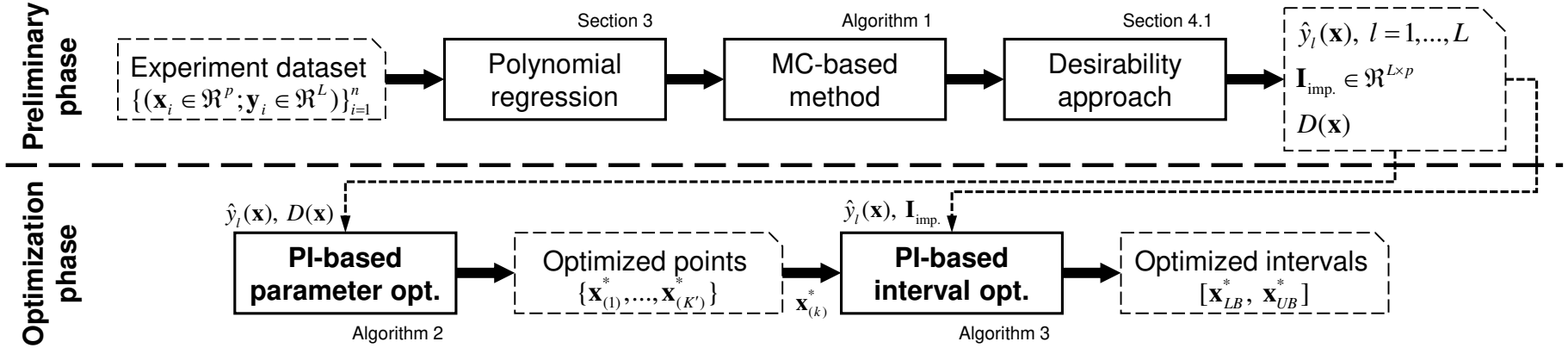

Fig. 1. Procedure for the proposed PI-based optimization methods for optimizing parameter points and intervals.

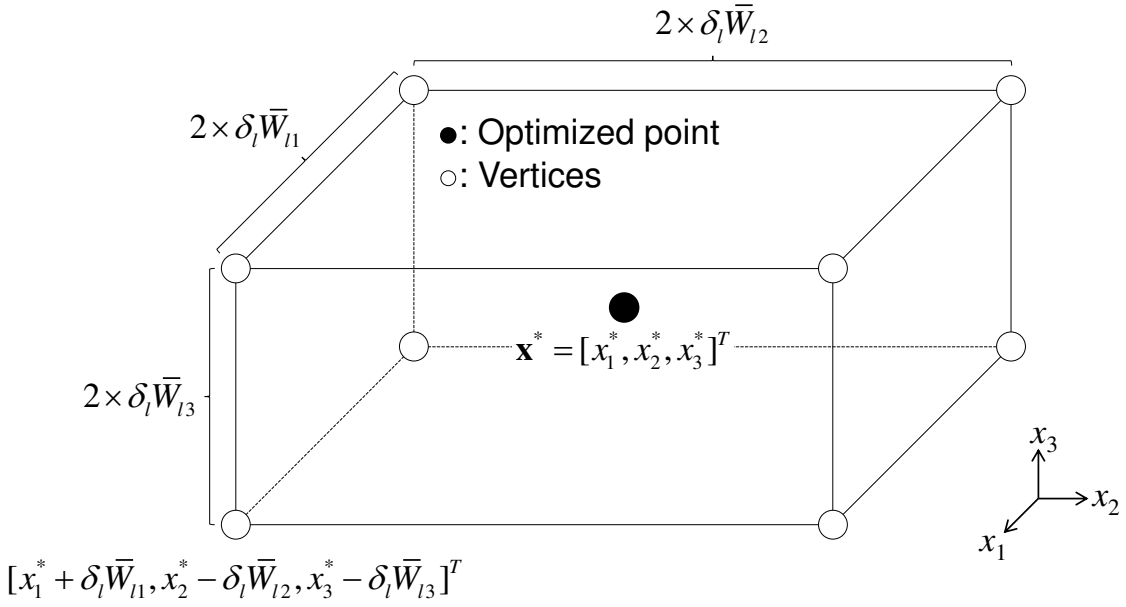

Fig. 2. Example of the hyper-rectangle defined in a three-dimensional input space.

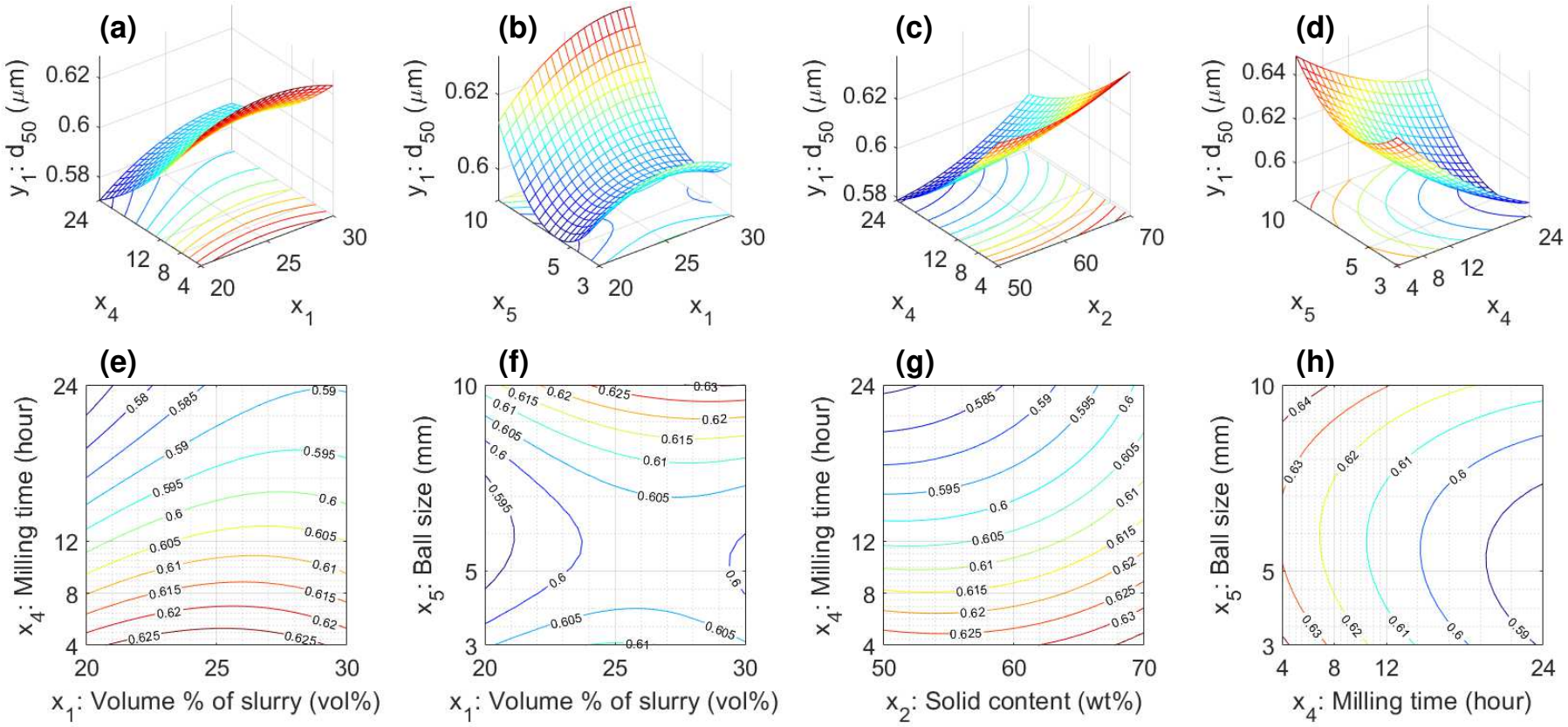

Fig. 3. Response surface plots (a-d) and contour plots (e-h) for the reduced model in eq. (10). For convenience of interpretations, the ranges of *X* and *Y* axes have been recovered from the range [−1, 1] to their original ranges.

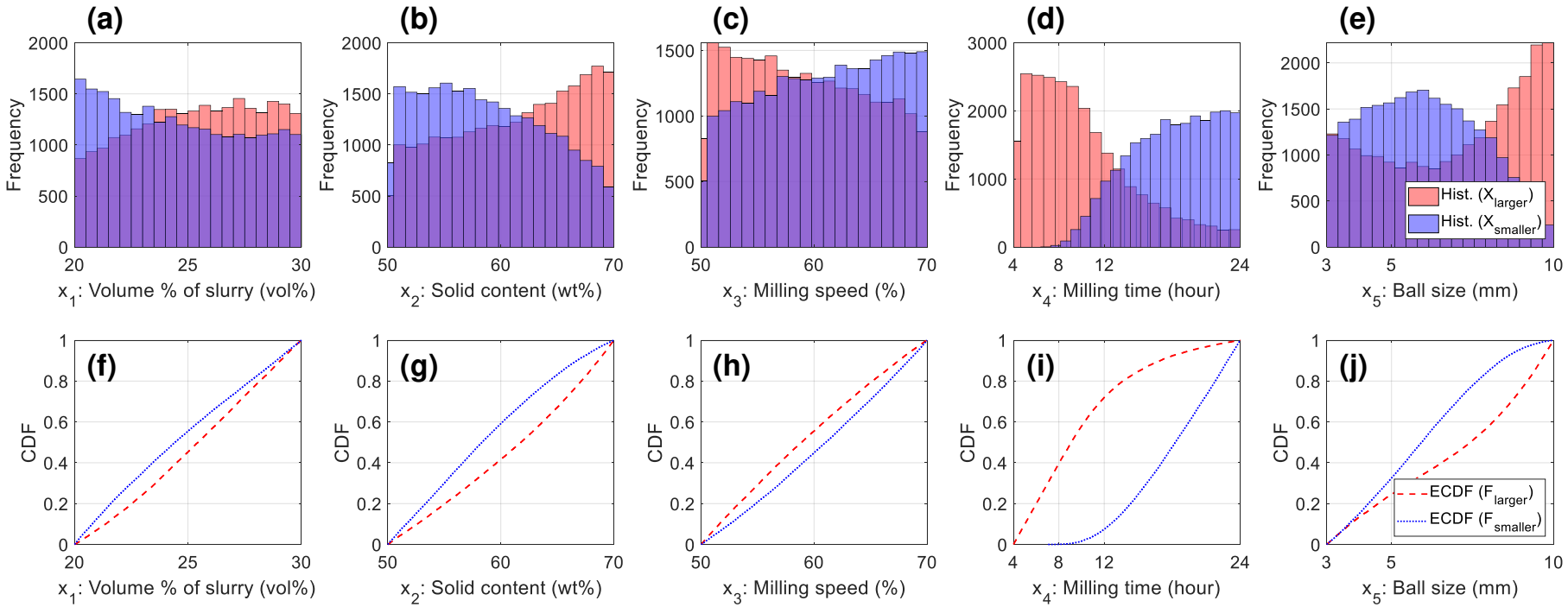

Fig. 4. Histograms of x_1,..., x_5 associated with X^1_{larger} and X^1_{smaller} (a-e) and estimated ECDFs $F^1_{\text{larger}}(x_j)$ and $F^1_{\text{smaller}}(x_j)$, j = 1,..., 5 (f-j). In Figs. 4 (a)-(e), for convenience of interpretations, the ranges of X axes have been recovered from the range [−1, 1] to their original ranges.

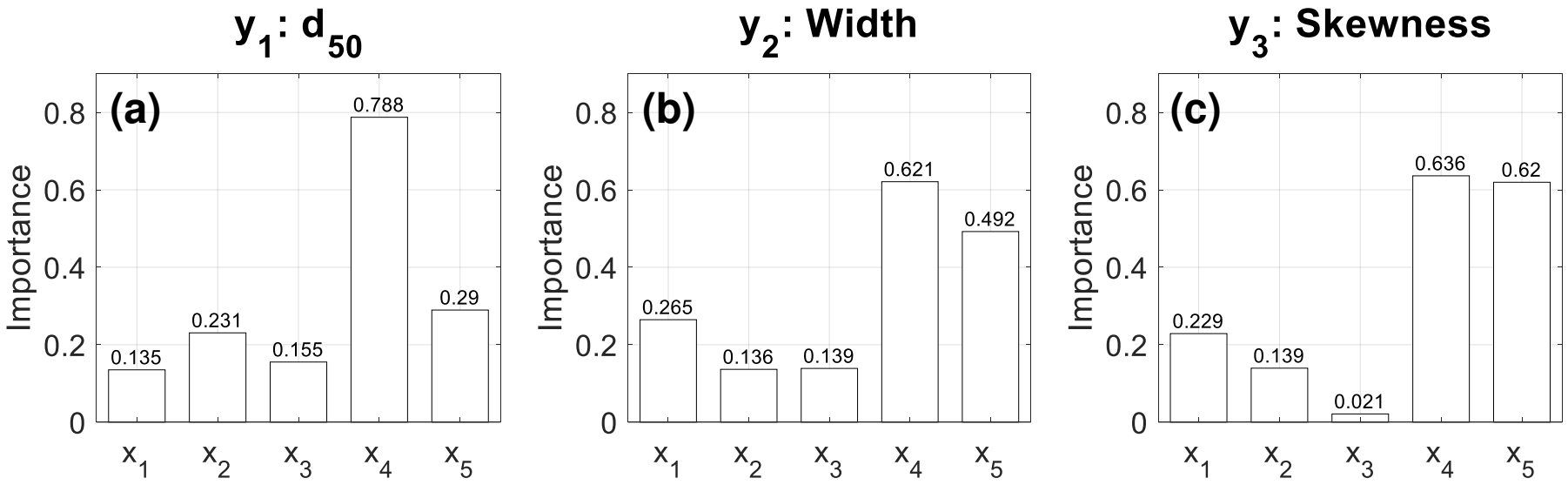

Fig. 5. Estimated importance values of x_1,..., x_5 for (a) y_1: d_{50}, (b) y_2: Width, and (c) y_3: Skewness.

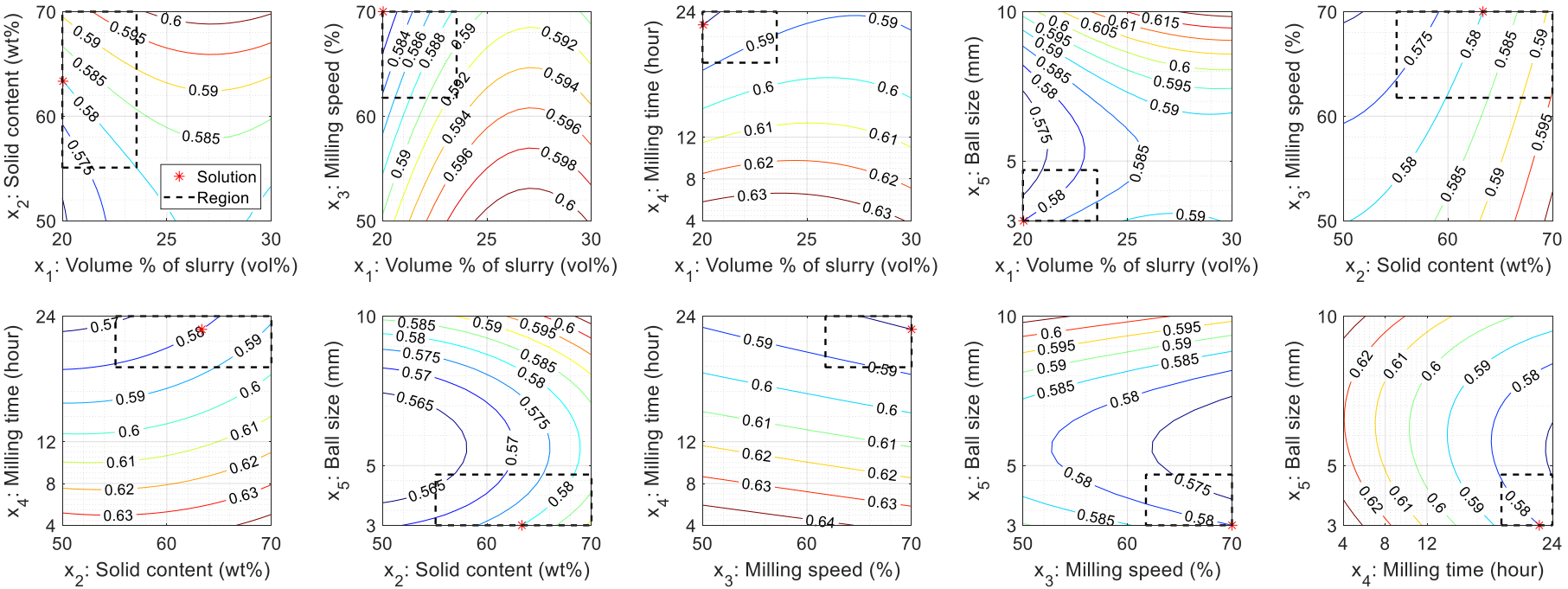

Fig. 6. Contour plots of $\hat{y}_1(\mathbf{x})$ with $\mathbf{x}^*_{(1)}$ in Table 3 and the input region defined by its optimized parameter intervals. For convenience of interpretations, the ranges of X and Y axes have been recovered from the range [−1, 1] to their original ranges.

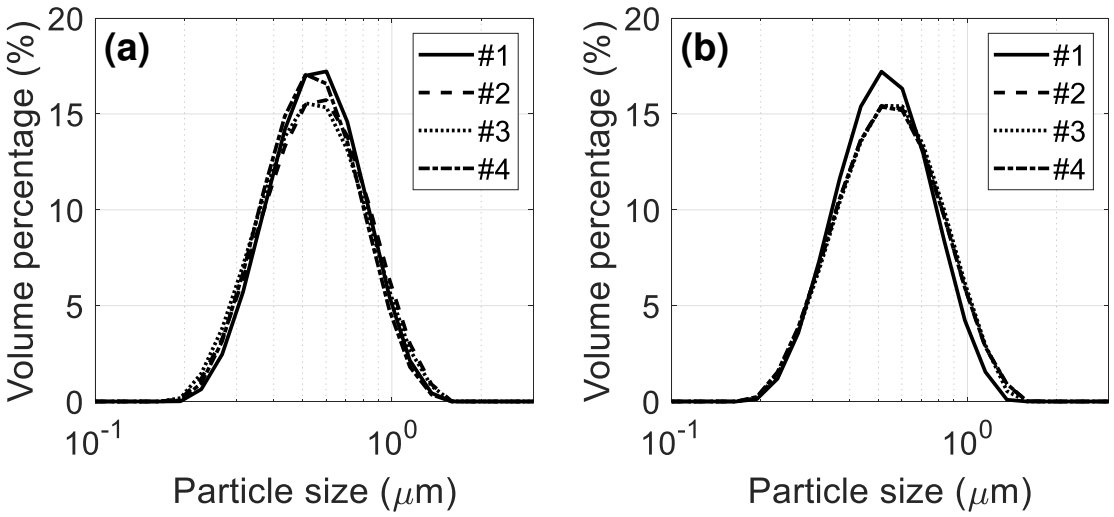

Fig. 7. PSDs of four milled powders in Tables 5 (a) and 6 (b).

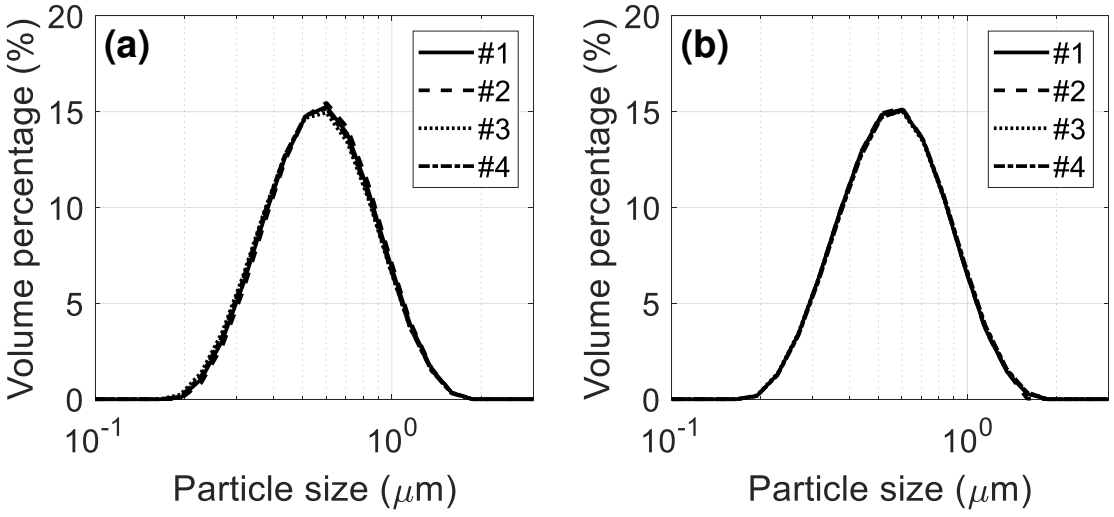

Fig. 8. PSDs of four milled powders in Tables 7 (a) and 8 (b).

Tables

Table 1. Statistically significant linear, interaction, and quadratic terms for each of quality responses. (Reproduced from our previous work, Ref. [37], copyright with permission from Elsevier).

Quality response	Statistically significant terms		
	Linear	Interaction	Quadratic
y_1: d_{50}	x_1, x_2, x_3, x_4, x_5	x_1x_4, x_1x_5, x_2x_4, x_4x_5	$x_1^2, x_2^2, x_4^2, x_5^2$
y_2: Width	x_1, x_2, x_3, x_4, x_5	x_2x_3, x_3x_5	x_4^2, x_5^2
y_3: Skewness	x_1, x_2, x_4, x_5	x_1x_5, x_2x_5, x_3x_5	$x_2^2, x_3^2, x_4^2, x_5^2$

Table 2. Performance indices of full and reduced models for three responses.

Performance Index	$\hat{y}_1(\mathbf{x})$		$\hat{y}_2(\mathbf{x})$		$\hat{y}_3(\mathbf{x})$	
	Full	Reduced	Full	Reduced	Full	Reduced
RMSE	0.0131	0.0131	0.135	0.134	0.0205	0.0202
R^2	0.753	0.742	0.759	0.747	0.867	0.864
Adjusted R^2	0.722	0.722	0.729	0.733	0.851	0.855
F-statistic	24.3	36.7	25	55.7	51.9	97.1

Table 3. ($y_{1,\text{target}}$ = 0.58 μm, $y_{2,\text{target}}$ = 'min', $y_{3,\text{target}}$ = 'min') Optimized parameter points by Algorithm 2 and their model outputs. The optimized parameter intervals by Algorithm 3 are presented at the bottom of the parameter values in $\mathbf{x}^*_{(1)}$ and $\mathbf{x}^*_{(3)}$.

Order	Optimized parameter point $\mathbf{x}^*$					Model output		
	x_1^*	x_2^*	x_3^*	x_4^*	x_5^*	$\hat{y}_1(\mathbf{x}^*)$	$\hat{y}_2(\mathbf{x}^*)$	$\hat{y}_3(\mathbf{x}^*)$
1	**20.03** **[20.00, 23.55]**	**63.34** **[55.09, 70.00]**	**70.00** **[61.77, 70.00]**	**22.74** **[19.12, 24.00]**	**3.00** **[3.00, 4.70]**	**0.580** **[0.544, 0.616]**	**1.102** **[0.744, 1.460]**	**0.239** **[0.184, 0.293]**
2	20.11	63.48	70.00	22.94	3.00	0.580 [0.544, 0.616]	1.102 [0.744, 1.460]	0.239 [0.184, 0.293]
3	**20.01** **[20.00, 23.42]**	**52.83** **[50.00, 60.83]**	**50.00** **[50.00, 57.98]**	**23.04** **[19.53, 24.00]**	**3.00** **[3.00, 4.65]**	**0.580** **[0.544, 0.616]**	**1.106** **[0.746, 1.465]**	**0.245** **[0.191, 0.300]**
4	20.00	52.81	50.00	23.01	3.00	0.580 [0.544, 0.616]	1.106 [0.746, 1.465]	0.245 [0.191, 0.300]
5	20.00	52.75	50.00	23.00	3.00	0.580 [0.544, 0.616]	1.105 [0.746, 1.465]	0.245 [0.191, 0.300]
6	20.00	52.58	50.00	22.97	3.00	0.580 [0.544, 0.616]	1.104 [0.745, 1.464]	0.245 [0.191, 0.300]
7	20.00	52.58	50.00	22.97	3.00	0.580 [0.544, 0.616]	1.104 [0.745, 1.464]	0.245 [0.191, 0.300]
8	20.00	52.55	50.00	22.97	3.00	0.580 [0.544, 0.616]	1.104 [0.745, 1.464]	0.245 [0.191, 0.300]
9	20.00	52.54	50.00	22.96	3.00	0.580 [0.544, 0.616]	1.104 [0.745, 1.464]	0.245 [0.191, 0.300]
10	20.00	52.43	50.00	22.95	3.00	0.580 [0.544, 0.616]	1.103 [0.744, 1.463]	0.246 [0.191, 0.300]

Table 4. ($y_{1,\text{target}}$ = 0.60 μm, $y_{2,\text{target}}$ = 'min', $y_{3,\text{target}}$ = 'min') Optimized parameter points by Algorithm 2 and their model outputs. The optimized parameter intervals by Algorithm 3 are presented at the bottom of the parameter values in $\mathbf{x}^*_{(1)}$ and $\mathbf{x}^*_{(9)}$.

Order	Optimized parameter point $\mathbf{x}^*$					Model output		
	x_1^*	x_2^*	x_3^*	x_4^*	x_5^*	$\hat{y}_1(\mathbf{x}^*)$	$\hat{y}_2(\mathbf{x}^*)$	$\hat{y}_3(\mathbf{x}^*)$
1	**22.00** **[20.00, 26.39]**	**63.40** **[53.04, 70.00]**	**50.00** **[50.00, 60.26]**	**20.67** **[16.00, 24.00]**	**3.00** **[3.00, 5.00]**	**0.600** **[0.565, 0.635]**	**1.219** **[0.863, 1.576]**	**0.252** **[0.198, 0.306]**
2	21.83	64.15	50.00	20.98	3.00	0.600 [0.565, 0.635]	1.219 [0.862, 1.576]	0.252 [0.198, 0.306]
3	21.73	63.75	50.00	20.62	3.00	0.600 [0.565, 0.635]	1.218 [0.861, 1.575]	0.252 [0.198, 0.306]
4	21.70	63.83	50.00	20.63	3.00	0.600 [0.565, 0.635]	1.218 [0.861, 1.575]	0.252 [0.198, 0.306]
5	21.79	64.35	50.01	21.06	3.00	0.600 [0.565, 0.635]	1.219 [0.862, 1.576]	0.252 [0.198, 0.306]
6	21.79	64.47	50.00	21.15	3.00	0.600 [0.565, 0.635]	1.219 [0.862, 1.576]	0.252 [0.198, 0.306]
7	21.63	62.90	50.00	20.02	3.00	0.600 [0.565, 0.635]	1.217 [0.860, 1.574]	0.252 [0.198, 0.307]
8	21.58	63.59	50.00	20.36	3.00	0.600 [0.565, 0.635]	1.217 [0.860, 1.574]	0.252 [0.198, 0.307]
9	**21.62** **[20.00, 24.70]**	**54.07** **[50.00, 61.32]**	**50.00** **[50.00, 57.18]**	**17.20** **[13.93, 20.46]**	**3.00** **[3.00, 4.45]**	**0.600** **[0.565, 0.635]**	**1.193** **[0.835, 1.552]**	**0.259** **[0.205, 0.313]**
10	21.53	63.82	50.00	20.45	3.00	0.600 [0.565, 0.635]	1.217 [0.860, 1.574]	0.252 [0.198, 0.307]

Table 5. Measured quality responses from four milled powders by $\mathbf{x}^{*}_{(1)}$ in Table 3.

Index	y_1: d_{50}	y_2: Width	y_3: Skewness
1	0.603	0.937	0.207
2	0.604	1.031	0.226
3	0.587	1.044	0.237
4	0.581	0.957	0.219
Average	0.594	0.992	0.222

Table 6. Measured quality responses from four milled powders by $\mathbf{x}^{*}_{(3)}$ in Table 3.

Index	y_1: d_{50}	y_2: Width	y_3: Skewness
1	0.567	0.951	0.217
2	0.589	1.054	0.237
3	0.593	1.042	0.230
4	0.588	1.060	0.239
Average	0.584	1.027	0.231

Table 7. Measured quality responses from four milled powders by $\mathbf{x}^{*}_{(1)}$ in Table 4.

Index	y_1: d_{50}	y_2: Width	y_3: Skewness
1	0.623	1.077	0.243
2	0.632	1.066	0.240
3	0.611	1.098	0.249
4	0.615	1.085	0.244
Average	0.620	1.082	0.244

Table 8. Measured quality responses from four milled powders by $\mathbf{x}^{*}_{(9)}$ in Table 4.

Index	y_1: d_{50}	y_2: Width	y_3: Skewness
1	0.611	1.079	0.241
2	0.610	1.080	0.244
3	0.611	1.097	0.251
4	0.616	1.099	0.253
Average	0.612	1.089	0.247